Supplementary Material:

Non-dispersive UV absorption spectroscopy: a promising new approach for in-situ detection of sulfur dioxide

1 SUPPLEMENTARY DATA

1.1 Analytical approximation of instrument response

According to the manuscript, the measured quantity in the PITSA is the integrated optical depth

$$\tau = -\log\left(\frac{I}{I_0}\right)$$
$$= -\log\left(\frac{\int I(\lambda)\,d\lambda}{\int I_0(\lambda)\,d\lambda}\right)$$
$$= -\log\left(\frac{\int I_0(\lambda)\cdot\exp(-\sigma(\lambda)\,L\,c)\,d\lambda}{\int I_0(\lambda)\,d\lambda}\right)$$

where in the last step, the Beer-Lambert law $I(\lambda) = I_0(\lambda)\cdot\exp\left(-\sigma(\lambda)\,c\,L\right)$ was inserted. For $\sigma(\lambda)\,c\,L \approx 0$, the exponential term can be linearly approximated according to $\exp(x) \approx 1 + x$, yielding

$$\tau \approx -\log\left(\frac{\int I_0(\lambda)\cdot(1-\sigma(\lambda)\,L\,c)\,d\lambda}{\int I_0(\lambda)\,d\lambda}\right)$$
$$= -\log\left(\frac{\int I_0(\lambda)\,d\lambda - L\,c\int I_0(\lambda)\,\sigma(\lambda)\,d\lambda}{\int I_0(\lambda)\,d\lambda}\right)$$
$$= -\log\left(\frac{I_0 - L\,c\int I_0(\lambda)\,\sigma(\lambda)\,d\lambda}{I_0}\right)$$
$$= -\log\left(1 - L\,c\int \frac{I_0(\lambda)}{I_0}\,\sigma(\lambda)\,d\lambda\right)$$

By defining the 'effective absorption cross section'

$$\sigma_{eff} = \int \frac{I_0(\lambda)}{I_0}\,\sigma(\lambda)\,d\lambda$$

and by linearly approximating the logarithm for $\sigma_{eff}\,L\,c \approx 0$ according to $\log(x) \approx x - 1$, yields the final result:

$$\tau = -\log\left(1 - \sigma_{eff}\,c\,L\right) \approx \sigma_{eff}\,L\,c$$

Appropriate limits of integration are discussed in the manuscript.

2 SUPPLEMENTARY TABLES AND FIGURES

2.1 Additional information on the PITSA setup
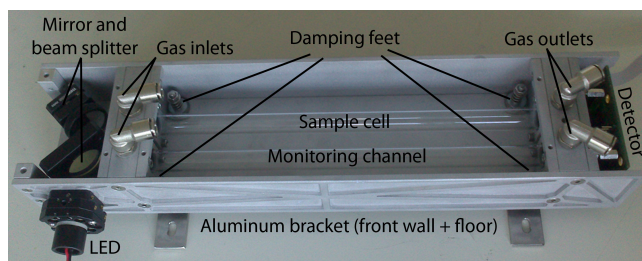

Figure S1. The optical bench (cover removed) of the PITSA instrument. Note, that in this setup the LED monitoring channel was equipped with a second equivalent measurement cell, which was used during lab experiments but not for the measurements presented in this article.
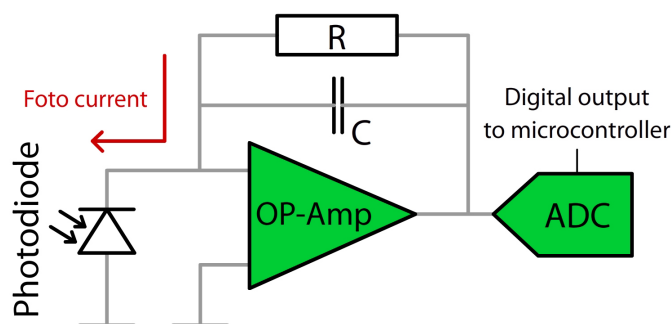

Figure S2. Simplified schematic of the detector electronics (one channel). The fotocurrent is converted to a few volt signal by a transimpedance amplification circuit, which was implemented using a chopper operational amplifier (OP-Amp). The value of the feedback resistor is $R = 3\,\text{M}\Omega$. The capacitance $C = 22\,\text{nF}$ was chosen, such that the time constant $\tau_{amp} = R\,C = 66\,\text{ms}$ of the amplifier is of the order of the minimum sampling time ($75\,\text{ms}$) of the analog-to-digital converter (ADC).

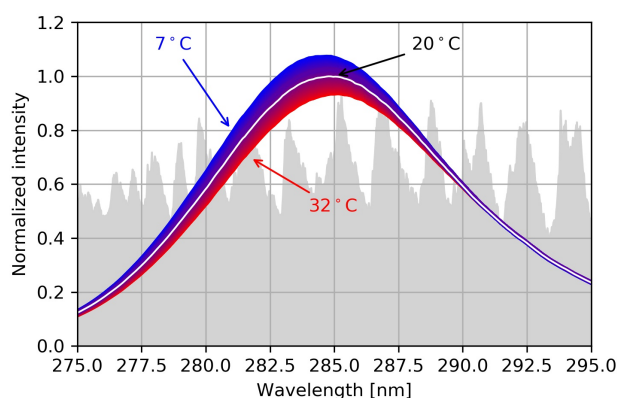## 2.2 Temperature dependence of the UV-LED spectrum

Figure S3. Spectra of the UV-TOP 280 at different temperatures. Note, that changes of the integrated intensity during operation of the PITSA are corrected by performing zero measurements, whereas changes in the spectral shape $\int I_0(\lambda)/I_0\,d\lambda$ are critical, since they lead to changes in the effective absorption cross section σ_{eff} and thus the instrument sensitivity. The latter comprises spectral shifts of the emission maximum and changes in the width.
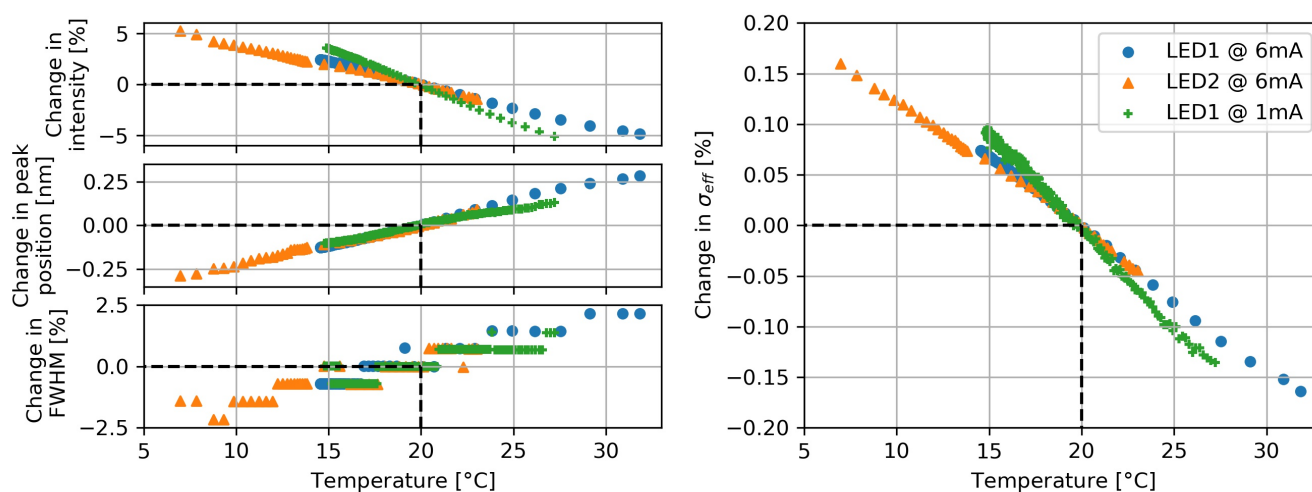

Figure S4. Separated investigation of the critical parameters: the intensity, the position of the emission maximum, the full width half maximum (FWHM) and the resulting effective absorption cross section σ_{eff}. Relative changes are given with respect to the spectrum recorded at $20\,°$C. Measurements were performed with two UV-TOP 280 LED's ('LED1' and 'LED2') and two supply currents ($6\,$mA and $1\,$mA). The trends basically follow linear trends. Extrapolation suggests, that at a supply current of $6\,$mA the effective absorption cross section changes by less than 1% over a temperature range from -10 to $50\,°$C.

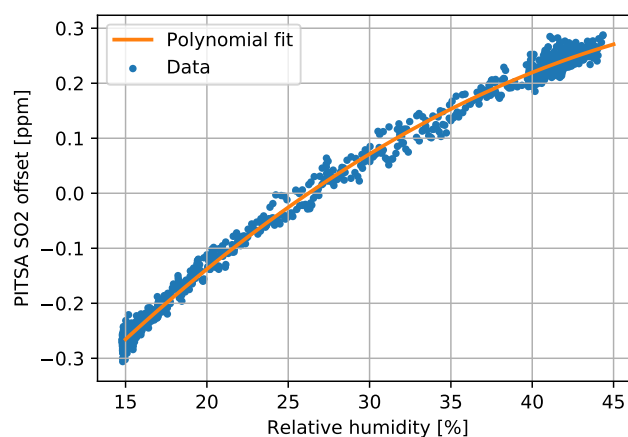## 2.3   Influence of relative humidity

Figure S5. Correlation of relative humidity and offset in the PITSA signal during zero measurements in an atmospheric simulation chamber. The correlation is stable in this particular case, since instrument and scrubber were running under comparatively stable lab conditions.